Evaluation of Enhanced Efficacy of COS-Based Ternary Blend Adsorbents for The Removal of Chromium and Copper from Wastewater

M. Sweety Chellam[1], A.Thaminum Ansari[2*] and P.N.Sudha[3]**

[1]PG Department of Chemistry, Voorhees College, (Affiliated to Thiruvalluvar University), Vellore – 632001, Tamilnadu, India

[2]PG & Research Department of Chemistry, Government Thirumagal Mills College, (Affiliated to Thiruvalluvar University), Gudiyattam, Vellore - 632602, Tamilnadu, India.

[3]Department of Physiology, Saveetha Dental College & Hospitals, Saveetha Institute of Medical and Technical Sciences (SIMATS), Saveetha University, Chennai -600077, Tamil Nadu, India

(Corresponding Authors: *Dr. A. Thaminum Ansari - thaminumansari731@gmail.com;

****Dr. P.N.Sudha – drparsu8@gmail.com)**

Abstract

A novel adsorbent derived from the naturally occurring biopolymers, chitosan oligosaccharide (COS), nanocrystalline cellulose (NCC), and polyethylene glycol (PEG) was synthesized using glutaraldehyde as a crosslinker to remove chromium and copper from aqueous solutions. The BET surface area analysis, FTIR, XRD, and SEM were used to describe the ternary blends, which were made in various ratios (1:1:1, 1:2:1, and 1:1:2). Variations in pH, adsorbent dose, contact time, and initial metal ion concentration were used to assess the COS/NCC/PEG-GLU blend's adsorption capability. The maximum adsorption capacity was attained at an adsorbent dosage of 5g, and the ideal pH for adsorption was determined to be 5. The adsorption capacity dropped as the starting metal ion concentration rose, and equilibrium was attained in 180 minutes. The Freundlich isotherm model provided the best description of the adsorption process, which followed pseudo-second-order kinetics. It was discovered that the maximal adsorption capabilities for Cu(II) and Cr(VI) were greater than 90%. Up to 99% of the adsorbed metals were recovered in desorption tests employing 0.1M HCl, demonstrating the adsorbent's capacity for regeneration. A promising environmentally friendly adsorbent for the removal of heavy metal ions from wastewater, the COS/NCC/PEG-GLU blend demonstrated exceptional adsorption capability.

Keywords: Chitosan oligosaccharide ternary blend, crosslinking, adsorption, heavy metals.

Introduction

Diseases that have varying consequences on the development and well-being of humans and animals are brought on by pollution from the buildup of chemicals, salts, heavy metals, and radioactive materials in soil and water (Basem et al., 2024). Large amounts of toxic pollutants, including dyes, heavy metal ions (copper, cadmium, lead, arsenic, and mercury), and others, are released into water bodies every day. These pollutants are extremely harmful to all living systems at concentrations higher than the WHO-recommended acceptable limits (Manzoor et al., 2019). One of the main contaminants found in industrial wastewater is heavy metals. All of the heavy metals, including lead, nickel, copper, chromium, mercury, and others, have the potential to cause extremely harmful impacts on living creatures. Mostly through plants and fish, heavy metals make their way into the food chain (Upadhyay et al., 2021).

Chromium, particularly in its hexavalent forms, stands out among heavy metal ions due to the fact that it is prevalent in groundwater contamination and because of the significant toxicity it possesses. Because these substances are responsible for a wide variety of diseases, ranging from cancer to skin blemishes, they present significant dangers to both aquatic life and human beings (Mohmoud and Ibrahim, 2023). It has been discovered that chromium (VI) is poisonous to humans, animals, plants, and microbes (Kozlowski and Walkowiak, 2002). Wilson disease, liver damage, and sleeplessness can all be brought on by copper from the electronics sector and device waste (Prabhu et al., 2017). Similar to this, other metals like zinc, chromium, and mercury are also extremely detrimental to living things, hence it is imperative that industrial effluent be properly treated before being released into the environment (Saha et al., 2019).

Numerous techniques, including ion exchange (Wang et al., 2018), reverse osmosis (Volpin et al., 2018), chemical precipitation (Charerntanyarak, 1999), solvent extraction (Hutton-Ashkenny et al., 2015), and membrane processes (Kirubanandam et al., 2023), are the methods for eliminating heavy metals from wastewater have been developed.

These procedures do have certain disadvantages, though. Their industrial use is limited by the fact that the majority of them are costly, time-consuming, produce sludge, require maintenance, and result in secondary pollutants. However, adsorption is a heavy metal removal technique that has garnered a lot of interest due to its affordability, ease of use, and effectiveness (Rekha at al., 2024). Since adsorption was identified as one of the most practical techniques for treating wastewater, scientists have been working tirelessly to create adsorbents that are affordable, efficient, environmentally benign, and repeatable.

In order to achieve environmental sustainability, biopolymers offer an alternate method of introducing surface hydrophilicity and biodegradability. Natural polymeric adsorbents are the best option because of their plentiful supply, low biological toxicity, and strong chemical modification capabilities (Verma et al., 2021). Biopolymers have emerged as the most promising products for the elimination of heavy metal ions in recent years due to their abundance, surface hydrophilicity, biodegradability, potential for cost-effective final product, and ability to be introduced for environmental sustainability. Many of the reactive groups found in natural polymers, particularly the easily accessible, affordable, and biodegradable polysaccharides such as chitosan, can take part in metal ion adsorption (Crini, 2005). However, chitosan cannot be used directly as an adsorbent due to its high crystallinity, low mechanical strength, and instability in an acidic medium. The main disadvantage of chitosan is its solubility in solutions with a pH of less than 4. Chitosan must therefore be improved to make it appropriate for adsorption (Vidal and Moraes, 2019). Hence efforts have been made to modify the same.

Chitosan oligosaccharide (COS) is a water-soluble polymer that is mostly produced by partially hydrolyzing chitosan, which is composed of two to ten glucosamine units that are connected by beta-1, 4-glycoside bonds (Kuroiwa et al., 2008). Chitosan oligosaccharide has drawn a lot more attention because it has unique physiological properties like antifungal and antibacterial activity, immunostimulating effects, and antitumor effects. It may also find use in the food, pharmaceutical, agricultural, and environmental sectors (Fernandez-de Castro et al., 2016; Ajitha et al., 2017).

The linear chain of cellulose is a polysaccharide made up of repeating units of β-(1→4)-D-glucopyranose. Strong intramolecular hydrogen connections are formed by these units, controlling the more crystalline properties of this extremely cohesive substance (Sayyed et al., 2021). These cellulosic materials can be transformed into cellulose nanocrystals for use in water treatment by applying mechanical or chemical pretreatments. These environmentally friendly nanoparticles are highly functional, have a large specific surface area, strong mechanical tolerance, and a highly biocompatible surface (Habibi et al., 2010). Hence the current study involved the use of nanocrystalline cellulose in the blend formation.

A petroleum-based polyether molecule with numerous uses is polyethylene glycol. It is regarded as one of the extremely investigated polyethers owing to its features like high hydrophilicity, remarkable biocompatibility, and non-immunogenicity, making it suitable for adsorption studies (Regev et al., 2019). Hence Polyethylene glycol is also used in the blend making in the current research. The backbones of several biopolymers, including chitosan,

nanocrystalline cellulose, polyethylene glycol, and the crosslinker glutaraldehyde, contain heteroatoms like nitrogen and oxygen that are used to modify their surfaces and improve their adsorption efficacy (Ahmad et al., 2017). Materials that are crosslinked have an amphiphilic nature. This property of these sorbents is what makes them so attractive; they have extremely hydrophobic sites that effectively trap nonpolar contaminants while also being sufficiently hydrophilic to swell significantly in water, enabling a quick diffusion process for the adsorbate (Joly et al., 2020). Hence in the present work, glutaraldehyde (GLU) crosslinked ternary blends of chitosan oligosaccharide (COS) with nanocrystalline cellulose (NCC) and polyethylene glycol PEG) of different ratios were prepared and utilized to remove copper and chromium, two heavy metals, from aqueous solutions by adsorptive mechanisms.

Materials and Methods

Materials

India Sea Foods, based in Cochin, Kerala, provided the chitosan oligosaccharide. PEG and glutaraldehyde were acquired from Central Drug House in New Delhi. We bought the cellulose powder from Himedia in Thane, India. For every other use, analytical-grade chemicals were used.

Preparation of Nanocrystalline cellulose (NCC)

50 ml of (1:2) H_2SO_4 was combined with 5 g of cellulose, and the mixture was stirred for an hour at 45 °C. In order to stop the acid hydrolysis process, 100 mL of cold water was added before centrifugation was used to separate the resulting CNCs. Several washing cycles were carried out until the pH reached neutral.

Preparation of the COS/NCC/PEG-Glu binary blend

One gram of chitosan oligosaccharide, one gram of NCC, and one gram of PEG were combined with a minimum of water and constantly agitated for about thirty minutes at room temperature. The homogenous solution was mixed with 7 mL of glutaraldehyde crosslinker and swirled continuously for two hours. To develop a ternary blend (1:1:1), the mixture was then transferred to a petri plate and dried using the crosslinker glutaraldehyde. Similarly blends with the ratios, 1:2:1 and 2:1:1 were also prepared in the same manner.

Characterization

FTIR Spectroscopy

FTIR spectra were obtained utilizing the KBr pellet technique in the 4000–400 cm-1 range using a Shimadzu IRAffinity-1S Spectrometer.

Powder X-ray Diffraction (XRD) studies

An X-ray powder diffractometer (XRD – SHIMADZU XD – D1) with a Ni-filtered Cu K α X-ray radiation source was used to assess the crystallinity of the prepared samples.

SEM and EDAX Analysis

High-resolution surface imaging can be achieved through the use of Scanning Electron Microscopy (SEM). The JEOL Model JSM-6390LV was used to examine the surface morphology at a magnification of X250. A 20 kV voltage was used to scan the material with an electron microscope.

Transmission electron microscopy (TEM) analysis

Nanocrystalline cellulose morphological data were obtained using a Transmission Electron Microscope (TEM) with a LaB6 JEM 2000 model, 2000 ×–1,500,000 × magnification, and 0.23 nm resolution.

Particle size and zeta potential measurement

Using N_2 adsorption/desorption isotherms and a NOVA-2200e, Quantachrome surface area analyzer, the Brunauer-Emmett Teller (BET) method was used to quantify the hydrogel's specific surface area, pore volume, and pore size.

Adsorption studies

The synthesized COS/NCC/PEG-Glu for the removal of Cr(VI) and Cu(II) from standard solutions were investigated using the batch adsorption method. The aqueous solutions of 200 ppm Cr (VI) and Cu (II) were prepared using deionized water for the adsorption studies. By shaking 1 gram of the hydrogel with 100 mL of stock solutions of Cr(VI) and Cu(II), the adsorption kinetics of the material were determined. When necessary, 2N HCL and 2N NaOH were used to make the initial pH changes. The pH-adjusted solution was kept in an orbital shaker set at 200 rpm for 60 minutes at 28^{o}C, which was the ideal contact time. The analysis was carried out according to the procedure. The Whatman filter paper was used to filter the reaction mixture after it had been shaken for an hour. AAS analysis was used to determine the solution's Cr (VI) and Cu (II) concentrations after filtering. The same methodology has been used to study changes in starting concentration, adsorbent dose, pH, and contact time. Following the completion of the adsorption process, the adsorption capacity (mg/g) and removal percentage (%) were calculated using the following formula. Following the completion of the adsorption process, the following equation was used to determine the removal percentage (%) and adsorption capacity (mg/g).

$$Removal\ (\%) = \frac{\text{Initial metal conc} - \text{Final metal conc}}{\text{Initial metal conc}} \times 100$$

Adsorption capacity (qe) = $\frac{C0-Ce \times V}{m}$

where the ultimate metal ion concentration is Ce, and the beginning concentration is Co. Where m is the dry adsorbent's weight in grams and V is the solution's volume in liters.

Isotherm Studies

The following equations give the linearized formula for the Langmuir and Freundlich isotherm models:

Langmuir equations:

$$\frac{C_e}{q_e} = \frac{1}{K_L q_m} + \frac{C_e}{q_m} \quad \text{----- (1)}$$

$$\frac{C_q}{C_{ad}} = C_q C_{max} + 1K_L C_{max} = K_L b \text{ ----------(2)}$$

Freundlich equation:

$$logq_e = logK_F + (1/n)logC_e \quad \text{----------(3)}$$

where Ce (mg/L) is the equilibrium concentration of Cr^{6+}, CrO_4^{2-}, and Cu^{2+} ions in aqueous solution, and qe (mg/g) is the amount of metal ions adsorbed at the equilibrium state. The maximal adsorption capacity of Cr^{6+}, CrO_4^{2-}, and Cu^{2+} ions is denoted by qm (mg/g). K_L and K_F (L/mg) are the constants for the Freundlich and Langmuir isotherm models, respectively. In the meantime, n represents the sorption intensity; if the n number is between 1 and 10, the sorption process will proceed easily. The qm and KL are determined by the intercepts and slopes of the straight lines on the Ce/qe versus Ce plot. The slope and intercept of log qe against the log Ce plot are used to calculate the values of 1/n and log K_F.

Desorption

0.1M HCL and 0.1M EDTA were added to the adsorbent to facilitate the desorption of the metal ions that were bound there. The metal-loaded adsorbent was subjected to individual processing with 100 mL of 0.1M HCL and 0.1M EDTA, and the aliquot was examined every 1, 2, 3, 4, and 5 hours. Using the following formula, the desorption ratio was determined from the quantity of metal ions adsorbed and the final concentration of metal ions in the desorption media.

$$Desorption\ Ratio = \frac{\text{Amount of metal ions desorbed}}{\text{Amount of metal ions adsorbed}} \times 100 \quad \text{---------- (4)}$$

Results and Discussion

Chitosan oligosaccharide, blends based on nanocellulose, and physical-methods-prepared composites feature unique functional groups, typically carboxyl (-COOH) and amino (-NH2), which allow for blends with high porosity and water absorption (Zhao et al., 2023). Using a physical crosslinking technique, Maiti et al. (2021) developed multicomponent chitosan-based blends and discovered that the carbonyl group (-C=O) of the added guar gum played a role in the crosslinking process. In the current study, a glutaraldehyde crosslinked ternary mix consisting of COS, NCC, and PEG was made using the sol-gel process and subjected to various experiments.

Surface properties

Surface area plays a crucial role in metal adsorption since it directly affects the number of adsorption sites available for metal ion binding. The adsorption capability is usually improved with surface area because there are more locations for metal ions to interact with. The pure COS and COS/NCC/PEG-GLU ternary blends were subjected to a BET surface area study at 77 K using Automatic BELSORP-mini II since the adsorbent's surface area is crucial to the adsorption process. The pore size and volume were estimated using the BJH method.

Table 1: Surface properties of the COS and the ternary blends

Sample	Parameters		
	Surface area (m^2/g)	Pore volume cc/g	Mean pore size (nm)
COS (Balaji et al., 2024)	97	0.1	92.03
COS/NCC/PEG-GLU (1:1:1)	184.45	0.93	4.25
COS/NCC/PEG-GLU (1:2:1)	124.27	0.32	6.15
COS/NCC/PEG-GLU (2:1:1)	152.61	0.78	9.33

The experimental findings showed that pure COS's pore volume and pore size were roughly 0.1 cc g-1 and 92.03 nm, respectively, and its surface area was 97 m^2 g^{-1}. The same batch of COS has been used in the present study also and in the crosslinked ternary blend (COS/NCC/PEG-GLU), surface area and pore volume increased as pore size decreased, according to comparisons with pure COS. The pore size has been 4.25nm, 6.25nm, and 9.33nm and surface area 184.45m^2/g, 124.27m^2/g, and 152.61m^2/g respectively for 1:1:1; 1:2:1, and 1:1:2 ratios, showing that the pore size was the minimum for 1:1:1 ratio which had the highest surface area of 184.45m^2/g making it more suitable for adsorption of metals. Similarly, Sherlala et al.

(2019) used a chitosan-magnetic graphene oxide (CS/MGO) composite with a surface area of 152.38 m2/g as an easily separable adsorbent for removing As(III) from an aqueous solution.

FTIR studies

Blends based on chitosan oligosaccharide and cellulose are promising biomaterials with strong uses in the cosmetics, absorbents, and medical fields. In the current research chitosan oligosaccharide was blended with nanocrystalline cellulose and polyethylene glycol in the presence of glutaraldehyde as a crosslinker.

FTIR analysis was used to establish the functional group profiles of the COS and COS/NCC/PEG-glu blends. **Table and Figures a,b,c and d** represent the FTIR spectra of COS and COS/NCC/PEG-glu; 1:1:1; 1:2:1 and 1:1:2 blends.

Table 2: Functional Group profiles of COS, COS/NCC/PEG -GLU blends

Functional groups	COS	COS/NCC/PEG -GLU blends		
		1:1:1	1:2:1	1:1:2
Bonded NH, CH, and OH stretching	3330, 2901	3399, 2938	3390,2933	3396,2935
Methyl group -C-H stretching		2867	2867	2866
	2039			
Carbonyl group	1633	1710	1665	1711
	1518		1561	1560
-C-O linkage	1396	1353, 1242	1351	1349
-C-O-C- linkage in polysaccharide	1079	1040	1036	1037

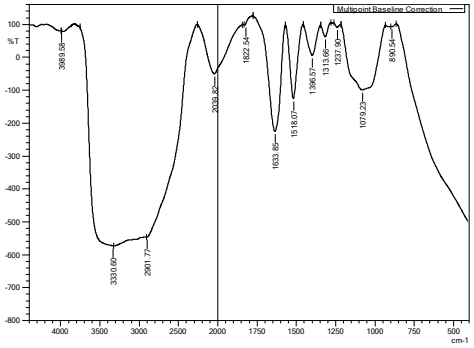

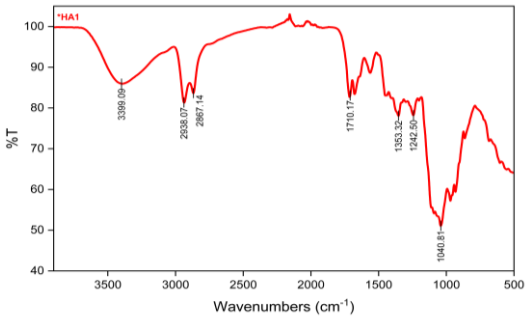

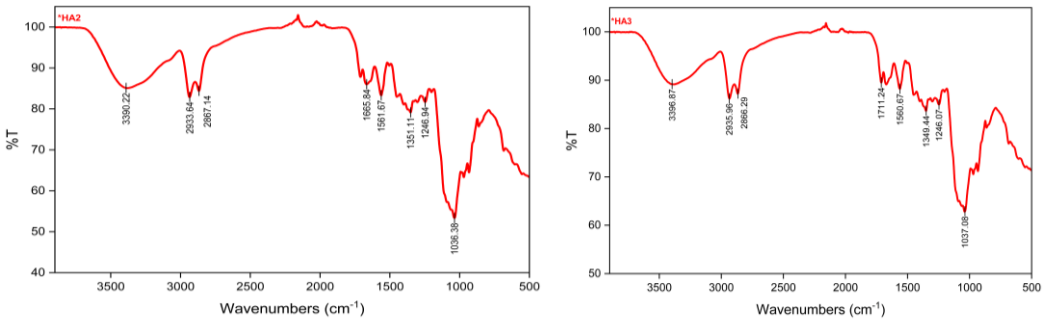

Figure 1: FTIR spectra of a) COS; b)COS/NCC/PEG-GLU1:1:1; c)COS/NCC/PEG-GLU 1:2:1; d) COS/NCC/PEG-GLU 1:1:2

FTIR of COS **(Figure ..)** showed peaks at 3330 cm^{-1} and 2901cm^{-1} for -OH stretching, -NH stretching and intermolecular hydrogen bonding, 1633cm^{-1} for -C=O carbonyl group, 1396cm^{-1} for -C-O linkage of alcohols and carbonyl groups, 1079$cm^{-1}$for -C-O-C linkage in polysaccharide proving the partially deacetylated amino polysaccharide, COS.

FTIR of **COS/NCC/PEG -GLU blend (1:1:1) (Figure)** showed peaks at 3399 cm^{-1}, and 2938 cm^{-1} are the stretching vibrational signals of -OH stretching, -NH stretching (Zeng et al., 2021) and intermolecular hydrogen bonding after blending and crosslinking, 2867cm^{-1} for methyl group C-H stretching of glutaraldehyde, 1710cm^{-1} for -C=N imine group (Monteiro Jr, and Airoldi, 1999), 1353cm^{-1}, and 1242cm^{-1} for -C-O linkage, 1040 cm^{-1} for -C-O-C linkage in polysaccharide (Luo et al., 2022). All the peaks had shifted either to higher or shorter wavenumbers, confirming that COS had effectively interacted with the -OH functional groups of NCC and PEG and also the -C=N imine groups due to the reaction of glutaraldehyde and the amino groups of COS. A similar shift in the wave numbers at 3390 cm^{-1}, 2933cm^{-1}, 3396 cm^{-1}, and 2935$cm^{-1}$for -OH stretching, -NH stretching, and intermolecular hydrogen bonding, 2867cm^{-1} and 2866cm^{-1} for methyl group C-H stretching of glutaraldehyde, 1665cm^{-1} and 1711cm^{-1} which are shifted to higher wavenumbers in -C=O of carbonyl groups of glutaraldehyde, at 1351cm^{-1} and 1349cm^{-1} for -C-O linkage and further peaks at 1036cm^{-1} and 1037cm^{-1} for -C-O-C linkage of polysaccharide of COS/NCC/PEG -GLU blend 1:2:1 and 1:1:2 respectively. Thus, the results of FTIR, confirm the formation of COS/NCC/PEG -GLU blends in different ratios.

X-Ray diffraction studies

The X-ray diffraction pattern of COS/NCC/PEG-GLU blends of ratios, 1:1:1; 1:2:1; 1:1:2 were recorded and shown in Figure .. .

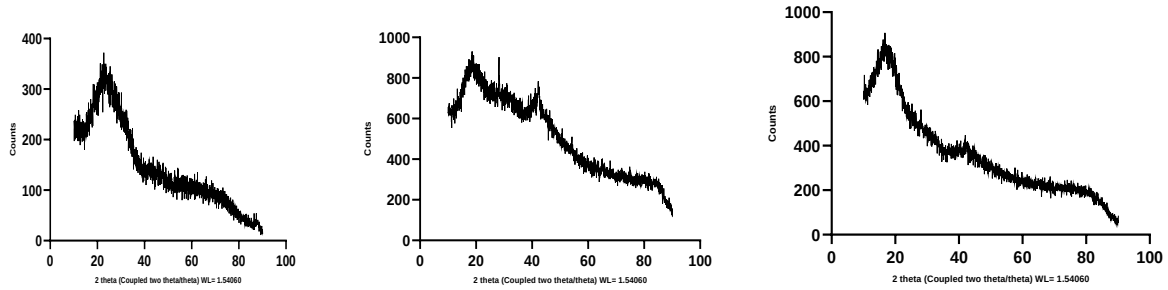

Figure 2: X Ray diffractograms of COS/NCC/PEG-GLU ratios[a)1:1:1b) 1:2:1 c) 1:1:2]

Table 3: Percentage Crystallinity of COS/NCC/PEG-GLU blends

Sample	2θ	% crystallinity
COS/NCC/PEG (1:1:1)	22	13
COS/NCC/PEG (1:2:1)	20, 42	41
COS/NCC/PEG (1:1:2)	20, 44	35

Sharp peaks were recorded at 22^{o}, 20^{o}, 42^{o,} and 20^{o}, 44^{o} in the above three blends with percentage crystallinity calculated as per the Nara and Komaiya (1983) method to be 13%, 41%, and 35% respectively. The results indicate that the percentage crystallinity of the ternary blend with a 1:1:1 ratio showed a very low crystallinity or more amorphous nature when compared to the 1:2:1 and 1:1:2 ratios. The higher percentage crystallinity of the 1:2:1 ratio may be due to the high content of nanocrystalline cellulose. It is always proved that the adsorption capacity decreases with increasing crystallinity (da Rocha et al., 2002; Wei et al., 2015). Hence among the three samples of different ratios of the ternary blends the 1:1:1 ratio with the very low crystallinity has a higher surface area as proved by the BET studies and should show better adsorption capacity. Hence this sample was used for the adsorption studies with heavy metals chromium and copper.

SEM Analysis

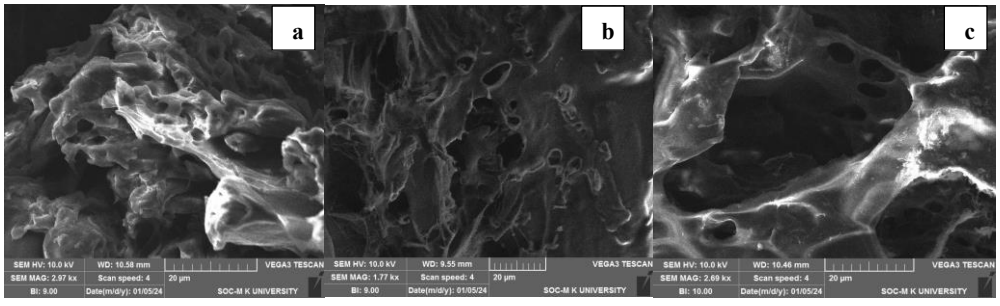

Figure 3: SEM Micrographs of COS/NCC/PEG-GLU ratios [a)1:1:1b) 1:2:1 c) 1:1:2]

The SEM images of the COS/NCC/PEG-GLU showed highly porous and rough surfaces with irregular shapes. In **Figures** (a, b, and c), in the regions where molecule aggregation was

significantly higher, a rough and porous surface structure was seen. Since the adsorbent's efficiency rose with decreasing particle size, this phenomenon made it possible for materials to have higher adsorption capacities. Porous materials having a large surface area have been found to be potential adsorbents for the adsorptive removal of heavy metals (Mondol, and Jhung, 2021).

TEM Studies

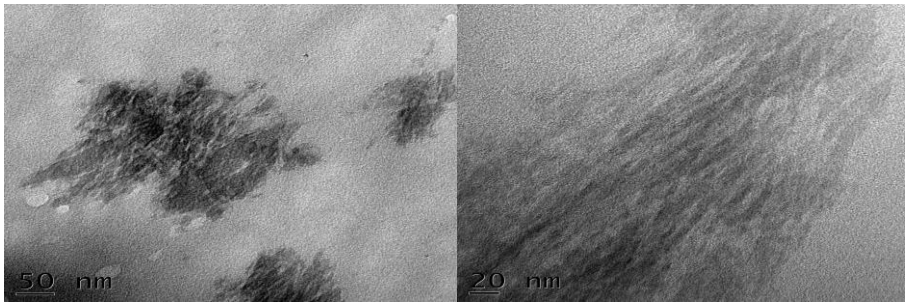

Figure 4: TEM images of Nanocrystalline Cellulose

Figure 4 shows the TEM micrograph images of Nanocrystalline Cellulose using LaB6 JEM 2000 model. Transmission electron microscopy images show the dispersion of nanocellulose crystals. The TEM image shows the NCC as a cylindrical, thread-like structure with a particle size range between 50 and 20 nm.

Adsorption Studies

Due to the adverse effects that environmental contamination of heavy metals is having on people all over the world, it is becoming a bigger issue. Metals are nonbiodegradable, insoluble, and bioaccumulated in both plants and mammals. Adsorption is a popular method for eliminating pollutants from industrial wastewater. Hence to remove heavy metals chromium and copper from aqueous solution, batch adsorption experiments were carried out using a thermostat shaker set to 200 rpm.

Effect of pH on the adsorption of Chromium and Copper

It has been shown that pH has a major effect on the adsorption of heavy metals onto various adsorbents. By regulating the degree to which basic and acidic compounds are ionised, pH affects absorption. Generally speaking, the initial pH level can either increase or decrease adsorption. This results from a change in the absorbent material's surface charge as the pH level varies (Al-Shemy et al., 2022)

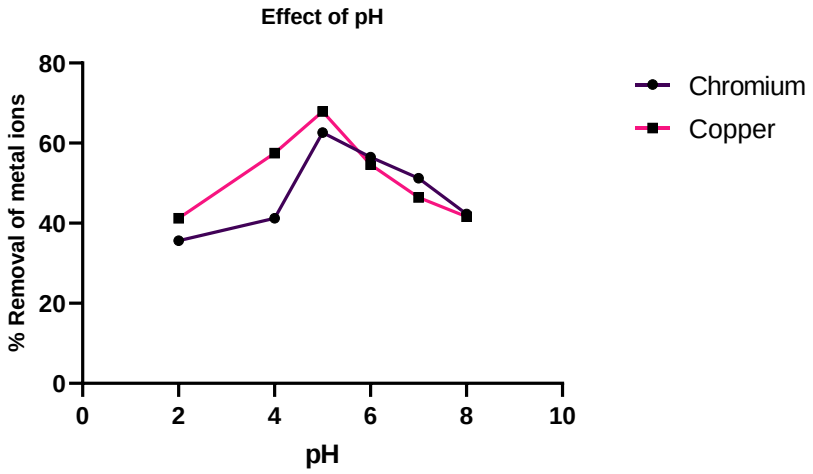

Figure 5: Effect of pH on the adsorption of Cr(VI) and Cu(II) ions

By affecting the adsorbent's surface characteristics and the adsorbate molecules' ability to associate or dissociate, a solution's pH is the primary factor that influences all other adsorption behaviour parameters (Vijayalakshmi et al., 2010). **Figure 5** displays how the adsorption of Cr(VI) and Cu(II) ions on COS/NCC/PEG-GLU varies with pH. As can be seen from the plot, the H3O+ ion concentration in the solution first drops as the pH rises from 2 to 5. This makes the adsorbent's surface more negatively charged, as indicated by zero-point charge, which raises the quantity of adsorption sites that are accessible. This leads to greater adsorption of both Cr(VI) and Cu(II) ions onto the adsorption sites, reaching maximum adsorption at pH 5. Nevertheless, raising the pH over 5 does not result in more metal ion adsorption, most likely because of equilibrium and competition between metal ions and H_3O^+. When the pH rises above 7.0, metal hydroxides—extremely persistent and preferentially formed—form, impairing the blend's binding properties and lowering adsorption (Kumar et al., 2012).

The electrostatic interaction between the metal ions and the negatively charged blend surface is the process by which Cr(VI) and Cu(II) are adsorbed onto the ternary blend. The surfaces of COS, NCC, and PEG all have hydroxyl and carbonyl functional groups. Electrostatic interaction, which is far stronger than van der Walls force, is often how these functional groups and heavy metal ions attach to one another.

Effect of adsorbent dose on the adsorption of Chromium and Copper

One important factor that has a big influence on the effectiveness and viability of the adsorption process is the dosage of the adsorbent. To examine the impact of adsorbent dosage, the temperature was maintained at 25◦C and the concentration was held steady at the ideal level of 200 mg/L. Adsorbent dosages ranging from 1g to 7g were investigated **(Figure 6).**

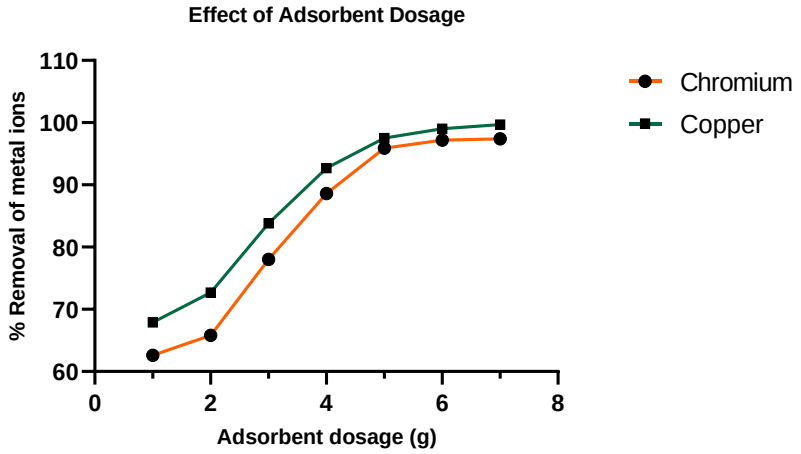

Figure 6: Effect of adsorbent dose on the adsorption of Cr(VI) and Cu(II) ions

As the adsorbent dose was increased from 1g to 5g, the absorption of both copper and chromium metals increased for all adsorbents under consideration, reaching its optimal value between 6g and 7g. These outcomes were anticipated since higher adsorbent dosages result in more active sites for adsorption, which increases metal removal (Azizi et al., 2024). According to the results, which are displayed in **Figure 6,** the removal effectiveness rose with dosage up to the "ideal dose," after which it stayed constant. This observation aligns with what other studies have found (Zhang et al., 2016; Islam et al., 2019; Ghosh et al., 2024). The ratio of adsorbed ions to the adsorbent mass decreases as dosage increases because fewer active adsorption sites are used. As a result, the adsorbent's capacity to adsorb is lowered (Khalil et al., 2020; Saini et al., 2023)

Effect of contact time on the adsorption of Chromium and Copper

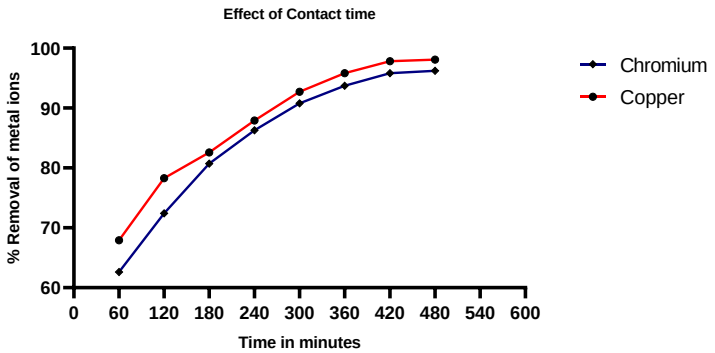

Figure 7: Effect of contact time on the adsorption of Cr(VI) and Cu(II) ions

The results showed that Cr(VI) and Cu(II) **(Figure 7)** are rapidly absorbed at the start of the reaction and continue to do so for 180 minutes. This is because the blend of material has a large number of vacant sites and open pores that are ideal for adsorbing Cr and Cu. The uptake achieves equilibrium after 180 minutes, and the adsorption capacity gradually increases.

However, the absence of an active site for metal ion adsorption onto the COS mixed material and a reduced driving energy are likely the causes of this rise. Consequently, 180 minutes was shown to be the optimal contact time for the subsequent trial.

Effect of initial metal ion concentration on the adsorption of Chromium and Copper

One important factor affecting the efficacy of adsorption is the initial concentration of metal ions (Abdelmonem et al., 2024). Using a series of batch tests, the effect of the initial metal concentration on the sorption of 1 g of the COS/NCC/PEG-Glu adsorbent is investigated.

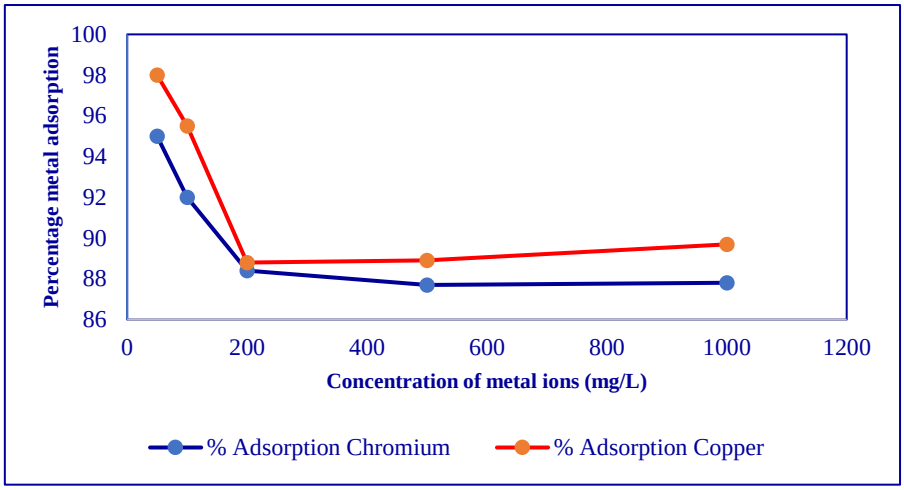

Figure 8: Effect of initial metal ion concentration on the adsorption of Cr(VI) and Cu(II) ions

From **Figure 8,** it may be concluded that while the adsorption rate remains high throughout the initial phase of adsorption, the solution ion removal rate progressively decreases as the solution ion concentration rises. This could be because, during the first low-concentration phase, the adsorbent's surface can offer sufficient active sites for copper ion adsorption. However, the adsorbent's active site remains constant as the concentration progressively rises, making it unable to provide more metal ions (Cui et al., 2024). Therefore, the adsorbent COS/NCC/PEG-GLU performs exceptionally well when treating wastewater that contains lower concentrations of copper and chromium ions. The mechanism of Cr(VI) and Cu(II) ion adsorption by the produced crosslinked ternary blend was clarified using Langmuir and Freundlich's isotherms.

Adsorption isotherms

The adsorption equilibrium isotherm describes the adsorbent's surface adsorption characteristics. The Freundlich model describes the multi-layer reversible adsorption process, while the Langmuir model assumes monomolecular layer adsorption, a homogeneous

adsorbent surface, no interaction between adsorbate molecules, and adsorption dynamic equilibrium (Guijarro-Aldaco et al.,2011; Cui et al., 2024).

Langmuir isotherm

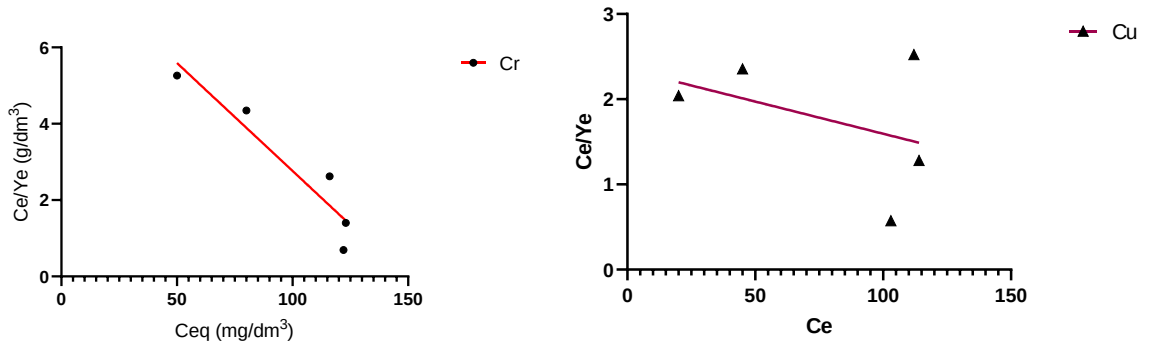

Freundlich Isotherm

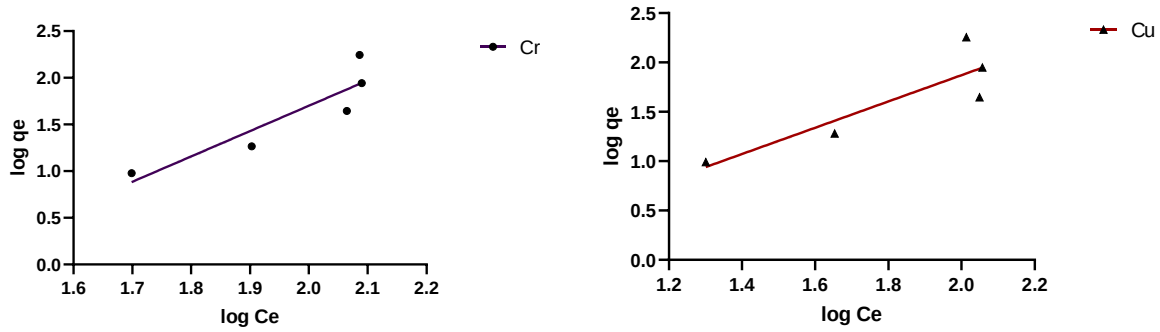

Figure 9: Langmuir and Freundlich plots for chromium and copper adsorption

Table 4: Langmuir and Freundlich constants for chromium and copper adsorption

Metal ions	Langmuir constants				Freundlich constants		
	K_L (dm^3/g)	b	C_{max}	R^2	K_F	n	R^2
Cr (VI)	0.8793	0.00671	131.04	0.9834	1.866	1.3682	0.9886
Cu (II)	0.95531	0.005633	169.59	0.9961	1.6188	1.5713	0.9981

The data was well-fitted by the curves derived from these models, suggesting that both models are capable of accurately describing the adsorption process by the synthesised ternary blend. In terms of fit, the Freundlich isotherm performed better than the Langmuir isotherm, indicating that both chemical and physical interactions contribute to adsorption (**Table 4 and Figure 9)**.

Adsorption Kinetics

Intraparticle diffusion kinetics, pseudo-first-order, and pseudo-second-order models were fitted to the experimental data in order to study the reaction of chromium and copper ion adsorption on the synthesised ternary blend. The plots are given below.

Pseudo First order (PFO) model

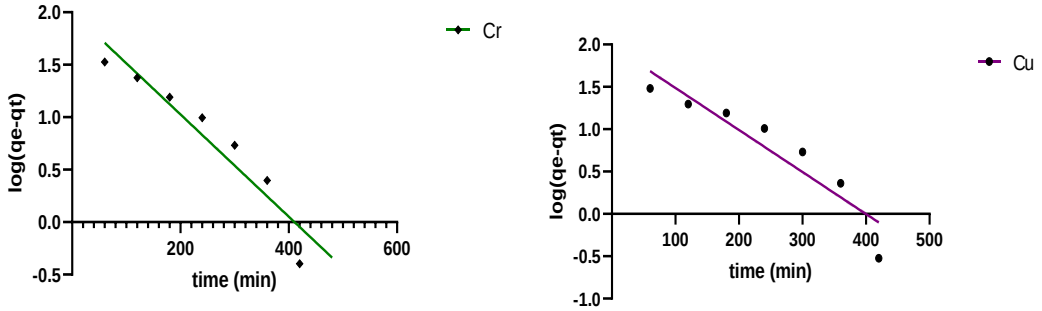

Pseudo Second order (PSO) model

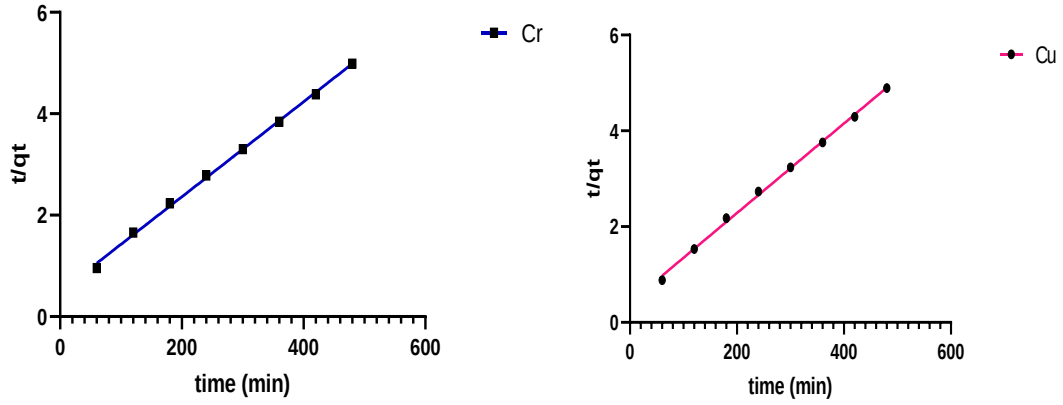

Intraparticle Diffusion (IPD) model

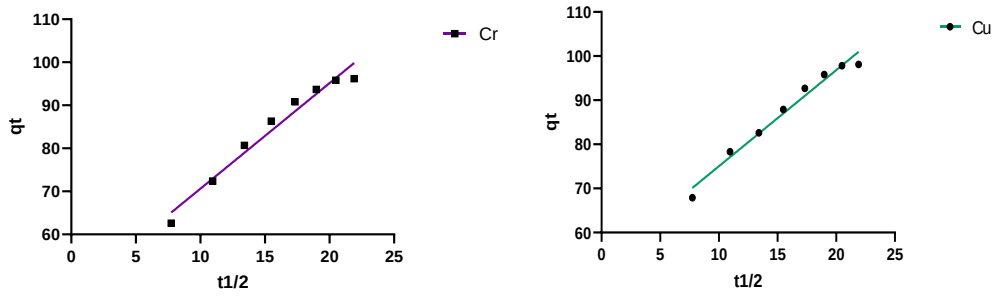

Figure 10: PFO, PSO, and IPD Intraparticle Diffusion (IPD) model plots of chromium and copper adsorption

Table 5: Kinetic data of adsorption of chromium and copper on COS/NCC/PEG-GLU blend

Metal ions	Pseudo-first-order kinetic model			Pseudo-second-order kinetic model			Intraparticle diffusion model		
	q_e (mg/g)	k_1 (min^{-1})	R^2	q_e (mg/g)	k_2 (g mg^{-1} min^{-1})	R^2	K_{id}	I	R^2
Cr(VI)	100.23	-0.011224	0.9053	106.76	0.0001793	0.9987	2.453	46.09	0.9672
Cu(II)	96.16	-0.011427	0.8705	106.96	0.000211018	0.9982	2.179	53.24	0.9753

According to the pseudo-first-order kinetic model **(Figure 10)**, the number of vacant active sites on the adsorbent surface determines the adsorption rate. By fitting the kinetics data to this model, the theoretical equilibrium capacity (qe) and pseudo-first-order rate constant (K1) for metal ions were found. The pseudo-second-order kinetic model, on the other hand, makes the assumption that chemisorption contributes to the adsorption process and that the concentration of metal ions in the solution and the availability of both adsorption sites control the adsorption rate.

When the correlation coefficients from the two kinetics models were compared, it was found that the pseudo-second-order kinetics correlation coefficient (R^2 -= 0.9987) was greater than the pseudo-first-order kinetics correlation coefficient (R^2 = 0.9053) **(Table 5).** As evidenced by its greater correlation coefficient, the pseudo-second-order kinetic is considered favored since it more accurately explains the experimental data. Because of the predominance of pseudo-second-order kinetics, the slower process of bond formation between the metal cation and the adsorbent's active sites—in this case, it is believed that the rate-limiting step in the adsorption process is the non-bonded electron pair of nitrogen in the amine groups.

The intra-particle diffusion model was used to analyze the kinetics results to comprehend the stages of diffusion mechanisms. The values of C were examined to gain an understanding of the boundary layer's thickness. It was discovered that the boundary layer's effect increased with the size of the intercept. In addition to internal adsorbent diffusion, the straight line's deviation from the origin in **Figure 10** suggests the existence of additional rate-controlling mechanisms. The reason that this straight-line deviates from the origin is due to the difference in the rate of mass transfer between the start and finish phases of adsorption (R^2 = 0.9753) (Ghosh et al., 2024). Hence the results confirm that the adsorption followed the PSO model.

Table 6: Comparison of COS-based blends on adsorption of heavy metals

Blend	Metal	C_{max}	Ref
COS-g-MA/PVA/SF	Pb	168.93	Ajitha et al., 2017
COS/PPG/Clay	Cu	142.68	Gopalakrishnan et al., 2018
EDTA-magnetic COS/CMC	Pb	432.34.	Lian et al., 2020
CS/ nano fibrillated cellulose aerogel	Pb	252.60	Upadhyay et al., 2021
COS/CMS	Cu	98.91	Balaji et al., 2021
COS/CMS/KC	Cu	132.45	Balaji et al., 2021
COS-g-GMA/PPG-Glu blend	Cd	99.08	Radha et al., 2021
COS/Salicylaldehyde Schiff base	Cu	110.00	Sharmila et al., 2024
COS/Salicylaldehyde Schiff base	Cr	120.00	Sharmila et al., 2024
COS/CMS-GLU	Pb	155.76	Balaji et al., 2024
COS/NCC/PEG-GLU	Cr	131.04	Present study
COS/NCC/PEG-GLU	Cu	169.59	Present study

Table 6 shows the list of chitosan oligosaccharide-based blends and composites reported for the removal of heavy metals copper, chromium, cadmium, and lead. The C_{max} values suggest that the chitosan oligosaccharide-based blends show very good adsorption capacity for various heavy metals which are similar to chitosan-based blends and composites. The adsorption capacity of the COS/NCC/PEG-Glu blend used in the current study also showed high C_{max} values of 131.04 and 169.59 for chromium and copper metals. This proves that the prepared crosslinked ternary blends show excellent adsorption capacity of heavy metals chromium and copper.

Studies have shown that the adsorption capacity of copper is indeed higher than that of chromium. This is because copper has a higher charge density and a more polarizable ion, making it more easily adsorbed onto the surface of adsorbents. For example, a study on the adsorption of copper and chromium onto activated carbon found that the copper adsorption capacity was significantly higher than that of chromium. This is likely due to the stronger electrostatic attraction between copper ions and the activated carbon surface.

Adsorption Mechanism

It was observed that both chemical and physical interactions are possible between the adsorbent and the metal ions. This suggests that the adsorption mechanism involves electrostatic interaction between the metal ion solution and the adsorption sites on different adsorbents (Shooto et al.,2019). This also assumed that the adsorption was chemisorption (Ahmad et al., 2020; Thabade et al., 2020). The coordination that also takes place during bond formation between the adsorbed substance and the adsorbent is responsible for the ternary blend's notable adsorption capacity for both metal ions. This illustrates how chemical adsorption, which creates a connection between the adsorbent and the transported metal ions (Cr^{6+} and Cu^{2+}), regulates the process. Both heavy metals can interact with NH_2, and OH groups

on the chitosan oligosaccharide, nanocrystalline cellulose, and polyethylene glycol structures leading to their adsorption. Similarly, the Freundlich adsorption isotherm is an empirical relationship that assumes chemisorption-type interaction between the adsorbent molecules and adsorbate. Its adsorption depends on heterogeneous locations. Additionally, it presumes that cations and anions adsorb on the adsorbent surfaces at the same time (Priyadarshini et al., 2024). It is also considered that the prepared ternary blend efficiently removes heavy metal ions by diffusion, adsorption, and forming a coordination complex with metal ions.

Desorption Studies

Large-scale adsorbent applications and the cost of the adsorption process are connected to whether or not the adsorbent can be regenerated. One of the most used techniques for adsorbent regeneration is the solvent method. In this study, 0.1MHCl was used as a desorbing agent and the mixture of the chromium and copper adsorbed ternary blends were shaken with the selected eluants, and the solution was drawn every one-hour up to 5 hours and the process was repeated for 3 cycles. The results are presented below.

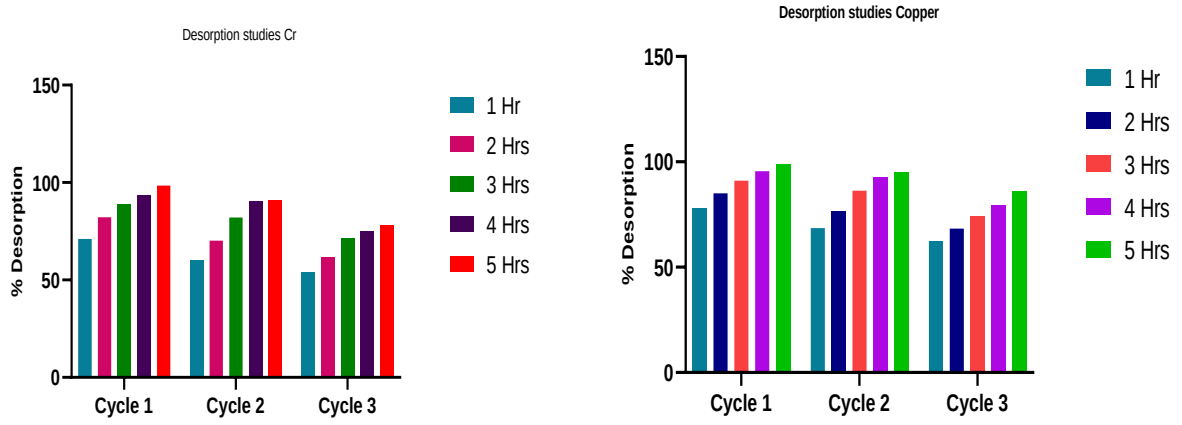

Figure 12: Desorption of Chromium and Copper

According to the study, the ternary blend's accumulated Cr(VI) and Cu(II) ions might be desorbed, resulting in the highest possible % recovery of these ions which was 98.4% and 99.0% with 0.1 M HCl in the first cycle which was 78.3% and 86.0% after 5^{th} hour in 3^{rd} cycle. The used HCl was found to regenerate the sorbent well releasing the metals. When the two metals were regenerated, the percentage regeneration of copper was found to be better when compared to chromium.

In general, regeneration is essential for increasing the adsorption process' economy and unlocking the adsorbent's potential for use in commercial settings. The best use of HCl as a desorbing agent proved that chemisorption along with physisorption had been the mechanism

of adsorption. Similar finding was recorded by by the desorption of Cr and Pb from the metals adsorbed groundnut husk by Bayuo et al., (2020). Similarly, using various acid-desorbing agents, Katsou et al. (2011) investigated the regeneration of natural zeolite contaminated by lead (II) and zinc (II) in wastewater treatment systems.

Conclusion

This study is unique in that it develops a crosslinked blend bio-adsorbent from COS, NCC, and PEG that effectively removes hazardous metal ions from manufacturing wastewater. The effectiveness of extracting Cr and Cu ions from a metal-loaded solution was also examined, as were the impacts of adsorption parameters like pH, adsorbent dosage, and initial metal ion concentration. The results show that pH, adsorbent dose, and time of contact significantly affect the adsorption performance of the adsorbent. A maximum of adsorption above 90% has been achieved. The type of interaction between the metals and the sorbent. The study's findings may aid in mitigating the detrimental effects of heavy metal contamination on the ecosystem and human well-being. The studies showed that the adsorbent could be very efficiently regenerated using HCl as the desorbing agent with 99% regeneration capacity. When considering the economic components of wastewater treatment, the chosen adsorbent is seen as a beneficial material. It accomplishes this by supporting the creation of an eco-friendly mixed adsorbent to remove heavy metal ions from water.

Declaration: The authors declare no conflict of interest.

References

- Abdelmonem, H. A., Hassanein, T. F., Sharafeldin, H. E., Gomaa, H., Ahmed, A. S., Abdel-lateef, A. M., ... & Tilp, A. H. (2024). Cellulose-embedded polyacrylonitrile/amidoxime for the removal of cadmium (II) from wastewater: Adsorption performance and proposed mechanism. *Colloids and Surfaces A: Physicochemical and Engineering Aspects*, *684*, 133081.
- Ahmad, A., Khan, N., Giri, B. S., Chowdhary, P., & Chaturvedi, P. (2020). Removal of methylene blue dye using rice husk, cow dung and sludge biochar: Characterization, application, and kinetic studies. *Bioresource Technology*, 306, 1–5. https://doi.org/10.1016/j.biortech.2020.123202

- Ahmad, M., Manzoor, K., Chaudhuri, R. R., & Ikram, S. (2017). Thiocarbohydrazide cross-linked oxidized chitosan and poly (vinyl alcohol): a green framework as efficient Cu (II), Pb (II), and Hg (II) adsorbent. *Journal of Chemical & Engineering Data*, *62*(7), 2044-2055. DOI: 10.1021/acs.jced.7b00088
- Ajitha, P., Vijayalakshmi, K., Saranya, M., Gomathi, T., Rani, K., Sudha, P. N., & Sukumaran, A. (2017). Removal of toxic heavy metal lead (II) using chitosan oligosaccharide-graft-maleic anhydride/polyvinyl alcohol/silk fibroin composite. *International journal of biological macromolecules*, *104*, 1469-1482.
- Al-Shemy, M. T., Al-Sayed, A., & Dacrory, S. (2022). Fabrication of sodium alginate/graphene oxide/nanocrystalline cellulose scaffold for methylene blue adsorption: Kinetics and thermodynamics study. *Separation and Purification Technology*, *290*, 120825.
- Azizi, S., Shaki, H., Shafeeyan, M. S., & Khonakdar, H. A. (2024). Chitosan-polyethylene oxide nanofiber/polyacrylamide-co-acrylic acid hydrogel nanocomposite: A copper ion adsorbent of aqueous solutions. *Inorganic Chemistry Communications*, *159*, 111682.
- Balaji, T. N., Rahman, S. M. A., Gomathi, T., Sudha, P. N., & Sheriff, A. K. S. I. (2021). Crosslinked chitosan oligosaccharide-based binary and ternary blends for the removal of Cu (II) ions. *International Journal of Environmental Science and Technology*, 1-12.
- Balaji, T. N., Venkatesh, K. S., Devanesan, S., AlSalhi, M. S., Vijayalakshmi, K., Prasad, P. S., ... & Sheriff, A. I. (2024). Removal of Pb (II) ions using chitosan oligosaccharide/carboxymethyl starch blend crosslinked with glutaraldehyde: a study on batch adsorption. *Polymer Bulletin*, *81*(17), 15727-15756.
- Basem, A., Jasim, D. J., Majdi, H. S., Mohammed, R. M., Ahmed, M., & Al-Rubaye, A. H. (2024). Adsorption of Heavy Metals from Wastewater by Chitosan: A Review. *Results in Engineering*, 102404.
- Bayuo, J., Abukari, M.A. & Pelig-Ba, K.B. Desorption of chromium (VI) and lead (II) ions and regeneration of the exhausted adsorbent. *Appl Water Sci* **10**, 171 (2020). https://doi.org/10.1007/s13201-020-01250-y
- Charerntanyarak, L. (1999). Heavy metals removal by chemical coagulation and precipitation. *Water Science and Technology*, *39*(10-11), 135-138. 10.1016/S0273-1223(99)00304-2
- Crini, G. (2005). Recent developments in polysaccharide-based materials used as adsorbents in wastewater treatment. *Progress in polymer science*, *30*(1), 38-70.

- Cui, J., Chen, H., Chen, Y., & Zhou, X. (2024). One step synthesis of carboxymethyl cellulose/graphene oxide composites for removal of copper ion from aqueous solution. *Diamond and Related Materials*, *150*, 111670.
- da Rocha, N. C., de Campos, R. C., Rossi, A. M., Moreira, E. L., Barbosa, A. D. F., & Moure, G. T. (2002). Cadmium uptake by hydroxyapatite synthesized in different conditions and submitted to thermal treatment. *Environmental science & technology*, *36*(7), 1630-1635.
- Fernandez-de Castro, L., Mengíbar, M., Sánchez, Á., Arroyo, L., Villarán, M. C., de Apodaca, E. D., & Heras, Á. (2016). Films of chitosan and chitosan-oligosaccharide neutralized and thermally treated: Effects on its antibacterial and other activities. *Lwt*, *73*, 368-374.
- Ghosh, A., Mondal, S., Kanrar, S., Srivastava, A., Pandey, M. D., Ghosh, U. C., & Sasikumar, P. (2024). Efficient removal of chromate from wastewater using a one-pot synthesis of chitosan cross-linked ceria incorporated hydrous copper oxide bio-polymeric composite. *International Journal of Biological Macromolecules*, *276*, 134016.
- Gopalakrishnan,M. Venkatesh, P., Gomathi, T. and Sudha, P.N. (2018). Preparation of chitosan oligosaccharide-based blends for the efficient extraction of heavy metal copper from wastewater. International Journal of Pharmacy and Biological Sciences. 8(4), 49-56.
- Guijarro-Aldaco, A., Hernández-Montoya, V., Bonilla-Petriciolet, A., Montes-Morán, M. A., & Mendoza-Castillo, D. I. (2011). Improving the adsorption of heavy metals from water using commercial carbons modified with egg shell wastes. *Industrial & engineering chemistry research*, *50*(15), 9354-9362.
- Habibi, Y., Lucia, L. A., & Rojas, O. J. (2010). Cellulose nanocrystals: chemistry, self-assembly, and applications. *Chemical reviews*, *110*(6), 3479-3500.
- Hutton-Ashkenny, M., Ibana, D., & Barnard, K. R. (2015). Reagent selection for recovery of nickel and cobalt from nitric acid nickel laterite leach solutions by solvent extraction. *Minerals Engineering*, *77*, 42-51.10.1016/j.mineng.2015.02.010
- Islam, M. N., Khan, M. N., Mallik, A. K., & Rahman, M. M. (2019). Preparation of bio-inspired trimethoxysilyl group terminated poly (1-vinylimidazole)-modified-chitosan composite for adsorption of chromium (VI) ions. *Journal of hazardous materials*, *379*, 120792.; 10.1016/j.jhazmat.2019.120792
- Joly, N., Ghemati, D., Aliouche, D., & Martin, P. (2020). Interaction of metal ions with mono-and polysaccharides for wastewater treatment: A review. *Nat. Prod. Chem. Res*, *8*(3), 373.

- Katsou E, Malamis S, Tzanoudaki M, Haralambous KJ, Loizidou M (2011) Regeneration of natural zeolite polluted by lead and zinc in wastewater treatment systems. J Hazard Mater 189(3):773–786. https://doi.org/10.1016/j.jhazmat-.2010.12.061
- Khalil, T. E., Elhusseiny, A. F., El-dissouky, A., & Ibrahim, N. M. (2020). Functionalized chitosan nanocomposites for removal of toxic Cr (VI) from aqueous solution. *Reactive and Functional Polymers*, *146*, 104407., 10.1016/j.reactfunctpolym.2019.104407
- Kirubanandam, S., Srinivasan, L., Alshalwi, M., Rajamanickam, A. K., & Narayanan, S. P. (2024). A novel organic–inorganic matrix nanofiltration membrane for remediating copper with enhanced thermal stability and mechanical strength. *Environmental Science and Pollution Research*, 1-16.
- Kozlowski, C. A., & Walkowiak, W. (2002). Removal of chromium (VI) from aqueous solutions by polymer inclusion membranes. *Water Research*, *36*(19), 4870-4876.
- Kumar, A. S. K.; Kalidhasan, S.; Rajesh, V.; Rajesh, N. Application of Cellulose-Clay Composite Biosorbent toward the Effective Adsorption and Removal of Chromium from Industrial Wastewater. *Ind. Eng. Chem. Res.* **2012**, *51*, 58– 69, DOI: 10.1021/ie201349h
- Kuroiwa, T., Noguchi, Y., Nakajima, M., Sato, S., Mukataka, S., & Ichikawa, S. (2008). Production of chitosan oligosaccharides using chitosanase immobilized on amylose-coated magnetic nanoparticles. *Process Biochemistry*, *43*(1), 62-69.
- Lian, Z., Li, Y., Xian, H., Ouyang, X. K., Lu, Y., Peng, X., & Hu, D. (2020). EDTA-functionalized magnetic chitosan oligosaccharide and carboxymethyl cellulose nanocomposite: Synthesis, characterization, and Pb (II) adsorption performance. *International Journal of Biological Macromolecules*, *165*, 591-600.
- Luo, Q., Ren, T., Lei, Z., Huang, Y., Huang, Y., Xu, D., ... & Wu, Y. (2022). Non-toxic chitosan-based hydrogel with strong adsorption and sensitive detection abilities for tetracycline. *Chemical Engineering Journal*, *427*, 131738.
- Mahmoud, M. E., & Ibrahim, G. A. (2023). Cr (VI) and doxorubicin adsorptive capture by a novel bionanocomposite of Ti-MOF@ TiO2 incorporated with watermelon biochar and chitosan hydrogel. *International Journal of Biological Macromolecules*, *253*, 126489.10.1016/j.ijbiomac.2023.126489
- Maiti, S., Khillar, P. S., Mishra, D., Nambiraj, N. A., & Jaiswal, A. K. (2021). Physical and self–crosslinking mechanism and characterization of chitosan-gelatin-oxidized guar gum hydrogel. *Polymer Testing*, *97*, 107155. 10.1016/j.polymertesting.2021.107155

- Manzoor, K., Ahmad, M., Ahmad, S., & Ikram, S. (2019). Synthesis, characterization, kinetics, and thermodynamics of EDTA-modified chitosan-carboxymethyl cellulose as Cu (II) ion adsorbent. *ACS omega*, *4*(17), 17425-17437.
- Mondol, M.M.H.; Jhung, S.H. Adsorptive removal of pesticides from water with metal–organic framework-based materials. *Chem. Eng. J.* **2021**, *421*, 129688.
- Monteiro Jr, O. A., & Airoldi, C. (1999). Some studies of crosslinking chitosan–glutaraldehyde interaction in a homogeneous system. *International journal of biological macromolecules*, *26*(2-3), 119-128.
- Nara S, Komiya TJSS (1983). Studies on the relationship between water-satured state and crystallinity by the diffraction method for moistened potato starch. Starch-Stärke 35(12):407-410. DOI:10.1002/STAR.19830351202
- Prabu, D.; Parthiban, R.; Ponnusamy, S. K.; Anbalagan, S.; John, R.; Titus, T. Sorption of Cu(II) Ions by Nano-Scale Zero Valent Iron Supported on Rubber Seed Shell. *IET Nanobiotechnol.* **2017**, *11*, 714– 724, DOI: 10.1049/iet-nbt.2016.0224.
- Priyadarshini, M., Rekha, E., Sathish, A., & Nithya, K. (2024). The relative performance of gelatin hydrogels doped with nanostructured transition-metal ferrites for chromium (VI) removal: Packed bed column studies and insights into reduction mechanisms. *Journal of Industrial and Engineering Chemistry*.
- Radha, E., Gomathi, T., Sudha, P. N., & Sashikala, S. (2021). Cadmium (II) ion removal from aqueous solution using chitosan oligosaccharide-based blend. *Polymer Bulletin*, *78*(2), 1109-1132.
- Regev, C., Belfer, S., Holenberg, M., Fainstein, R., Parola, A. H., & Kasher, R. (2019). Fabrication of poly (ethylene glycol) pa2015rticles with a micro-spherical morphology on polymeric fibers and its application in high flux water filtration. *Separation and Purification Technology*, *210*, 729-736.
- Rekha, A., Vijayalakshmi, K., Alswieleh, A., Sudha, P. N., Rani, J., & Vidhya, A. (2024). Enhanced removal of Cr (VI) from water using alginate-modified algal biochar: a promising adsorbent. *Biomass Conversion and Biorefinery*, 1-14.
- Saha, S., Zubair, M., Khosa, M. A., Song, S., & Ullah, A. (2019). Keratin and chitosan biosorbents for wastewater treatment: a review. *Journal of Polymers and the Environment*, *27*, 1389-1403.10.1007/s10924-019-01439-6

- Saini, P., Sowmya, C., Purnima, D., & Singh, S. A. (2023). Optimization of different polymer composites films for the removal of chromium. *Materials Today: Proceedings*, *72*, 192-198.
- Sayyed, A. J., Pinjari, D. V., Sonawane, S. H., Bhanvase, B. A., Sheikh, J., & Sillanpää, M. (2021). Cellulose-based nanomaterials for water and wastewater treatments: A review. *Journal of Environmental Chemical Engineering*, *9*(6), 106626.
- Sharmila, K., Srinivasan, L., Vijayalakshmi, K., Alshalwi, M., Alotaibi, K. M., Sudha, P. N., ... & Deepa, M. (2024). Evaluation of efficacy of chitosan oligosaccharide-salicylaldehyde Schiff base to extract copper (II) and chromium (VI) from synthetic wastewater. *Biomass Conversion and Biorefinery*, 1-16.
- Sherlala, A. I. A., Raman, A. A. A., Bello, M. M., & Buthiyappan, A. (2019). Adsorption of arsenic using chitosan magnetic graphene oxide nanocomposite. *Journal of environmental management*, *246*, 547-556.
- Shooto, N. D., Naidoo, E. B., & Maubane, M. (2019). Sorption studies of toxic cations on ginger root adsorbent. *Journal of Industrial and Engineering Chemistry*, 76, 133–140. https://doi.org/10.1016/j.jiec.2019.02.027
- Thabede, M. P., Shooto, N. D., Xaba, T., & Naidoo, E. B. (2020). Adsorption studies of toxic cadmium(II) and chromium(VI) ions from aqueous solution by activated black cumin (Nigella sativa) seeds. *Journal of Environmental Chemical Engineering*, 8(4), 1–12. https://doi.org/10.1016/j.jece.2020.104045
- Upadhyay, U., Sreedhar, I., Singh, S. A., Patel, C. M., & Anitha, K. L. (2021). Recent advances in heavy metal removal by chitosan-based adsorbents. *Carbohydrate Polymers*, *251*, 117000.
- Verma, M., Lee, I., Hong, Y., Kumar, V., & Kim, H. (2022). Multifunctional β-Cyclodextrin-EDTA-Chitosan polymer adsorbent synthesis for simultaneous removal of heavy metals and organic dyes from wastewater. *Environmental Pollution*, *292*, 118447.10.1016/j.envpol.2021.118447
- Vidal, R. R. L., & Moraes, J. S. (2019). Removal of organic pollutants from wastewater using chitosan: a literature review. *International journal of environmental science and technology*, *16*(3), 1741-1754.10.1007/s13762-018-2061-8
- Vijayalakshmi, P.; Bala, V. S. S.; Thiruvengadaravi, K. V.; Panneerselvam, P.; Palanichamy, M.; Sivanesan, S. Removal of Acid Violet 17 from Aqueous Solutions by Adsorption onto

Activated Carbon Prepared from Pistachio Nut Shell. *Sep. Sci. Technol.* **2010**, *46*, 155– 163, DOI: 10.1080/01496395.2010.484006

- Volpin, F., Fons, E., Chekli, L., Kim, J. E., Jang, A., & Shon, H. K. (2018). Hybrid forward osmosis-reverse osmosis for wastewater reuse and seawater desalination: Understanding the optimal feed solution to minimise fouling. *Process Safety and Environmental Protection*, *117*, 523-532.10.1016/j.psep.2018.05.006
- Wang, M., Payne, K. A., Tong, S., & Ergas, S. J. (2018). Hybrid algal photosynthesis and ion exchange (HAPIX) process for high ammonium strength wastewater treatment. *Water research*, *142*, 65-74.10.1016/j.watres.2018.05.043
- Wei, W., Yang, L., Zhong, W., Cui, J., & Wei, Z. (2015). Mechanism of enhanced humic acid removal from aqueous solution using poorly crystalline hydroxyapatite nanoparticles. *Digest Journal of Nanomaterials and Biostructures*, *10*(2), 663-680.
- Zeng, H., Hu, Z., Peng, C., Deng, L., & Liu, S. (2021). Effective adsorption and sensitive detection of Cr (VI) by chitosan/cellulose nanocrystals grafted with carbon dots composite hydrogel. *Polymers*, *13*(21), 3788.
- Zhang, L., Luo, H., Liu, P., Fang, W., & Geng, J. (2016). A novel modified graphene oxide/chitosan composite used as an adsorbent for Cr (VI) in aqueous solutions. *International journal of biological macromolecules*, *87*, 586-596.10.1016/j.ijbiomac.2016.03.027
- Zhao, C., Liu, G., Tan, Q., Gao, M., Chen, G., Huang, X., ... & Xu, D. (2023). Polysaccharide-based biopolymer hydrogels for heavy metal detection and adsorption. *Journal of Advanced Research*, *44*, 53-70.